NASA TECHNICAL NOTE

NASA TN D-7736

NASA TN D-7736

PRESSURE-VISCOSITY MEASUREMENTS FOR SEVERAL LUBRICANTS TO 5.5×10^8 NEWTONS PER SQUARE METER (8×10^4 PSI) AND 149° C (300° F)

by William R. Jones, Jr., Robert L. Johnson, Ward O. Winer, and David M. Sanborn

Lewis Research Center
Cleveland, Ohio 44135

NATIONAL AERONAUTICS AND SPACE ADMINISTRATION • WASHINGTON, D. C. • AUGUST 1974

1. Report No.	2. Government Accession No.	3. Recipient's Catalog No.
NASA TN D-7736		

4. Title and Subtitle	5. Report Date
PRESSURE-VISCOSITY MEASUREMENTS FOR SEVERAL LUBRICANTS TO 5.5×10^8 NEWTONS PER SQUARE METER (8×10^4 PSI) AND 149° C (300° F)	August 1974
	6. Performing Organization Code

7. Author(s)	8. Performing Organization Report No.
William R. Jones, Jr., Robert L. Johnson, Lewis Research Center; Ward O. Winer, and David M. Sanborn, Georgia Institute of Technology, Atlanta, Georgia	E-7952

9. Performing Organization Name and Address	10. Work Unit No.
Lewis Research Center National Aeronautics and Space Administration Cleveland, Ohio 44135	501-24
	11. Contract or Grant No.

12. Sponsoring Agency Name and Address	13. Type of Report and Period Covered
National Aeronautics and Space Administration Washington, D.C. 20546	Technical Note
	14. Sponsoring Agency Code

15. Supplementary Notes

16. Abstract

A capillary viscometer was used to measure viscosity as a function of pressure, temperature, and shear stress for a number of lubricants. Measurements were made at 38°, 99°, and 149° C (100°, 210°, and 300° F), gage pressure to 5.5×10^8 N/m^2 (8×10^4 psi), and shear stresses to 10^5 N/m^2 (14.5 psi). At 38° C (100° F), the order of the pressure-viscosity coefficients for the unformulated fluids was: fluorinated polyether > synthetic hydrocarbon > naphthenic mineral oil > synthetic paraffinic oil (lot 4) > C-ether ≅ synthetic paraffinic oil (lot 3) > polyalkyl aromatic > advanced ester. All pressure-viscosity coefficients decreased with increasing temperature. Fair agreement was obtained when pressure-viscosity coefficients at 38° C (100° F) and 6.9×10^7 N/m^2 (10^4 psi) were compared to data from other investigators using different techniques (optical elastohydrodynamics, oscillating crystal, and low shear capillary viscometry).

17. Key Words (Suggested by Author(s))	18. Distribution Statement
Elastohydrodynamic lubrication Pressure viscosity Liquid lubricants Lubricant rheology	Unclassified - unlimited Category 15

19. Security Classif. (of this report)	20. Security Classif. (of this page)	21. No. of Pages	22. Price*
Unclassified	Unclassified	37	$3.25

* For sale by the National Technical Information Service, Springfield, Virginia 22151

PRESSURE-VISCOSITY MEASUREMENTS FOR SEVERAL LUBRICANTS TO 5.5×10^8 NEWTONS PER SQUARE METER (8×10^4 PSI) AND 149° C (300° F)

by William R. Jones, Jr., Robert L. Johnson, Ward O. Winer,* and David M. Sanborn

Lewis Research Center

SUMMARY

A high-pressure capillary viscometer was used to measure viscosity as a function of pressure, temperature, and shear stress for a number of liquid lubricants. Measurements were made at 38°, 99°, and 149° C (100°, 210°, and 300° F), gage pressures to 5.5×10^8 N/m^2 (8×10^4 psi), and shear stresses to 10^5 N/m^2 (14.5 psi). Pressure-viscosity coefficients, expressed as reciprocal asymptotic isoviscous pressure α^* were determined for the test fluids. At 38° C (100° F) the order of the pressure-viscosity coefficients for the unformulated fluids was as follows: fluorinated polyether > synthetic hydrocarbon (traction fluid) > super-refined naphthenic mineral oil > synthetic paraffinic oil (lot 4) > C-ether ≅ synthetic paraffinic oil (lot 3) > polyalkyl aromatic > advanced ester. All pressure-viscosity coefficients decreased with increasing temperature.

The elastohydrodynamic (EHD) film forming capability of the test fluids was determined by the product of the pressure-viscosity coefficient and the atmospheric viscosity $\alpha^*\mu_0$. At 38° C (100° F) the order of the EHD film forming capability for the unformulated fluids was as follows: fluorinated polyether ≅ synthetic paraffinic oil (lot 4) ≅ synthetic paraffinic oil (lot 3) > super-refined naphthenic mineral oil > synthetic hydrocarbon (traction fluid) > C-ether > polyalkyl aromatic > advanced ester.

Fair agreement was obtained when pressure-viscosity coefficients at 38° C (100° F) and 6.9×10^7 N/m^2 (10^4 psi) were compared to data from other investigators using different techniques (optical elastohydrodynamics, oscillating crystal, and low shear capillary viscometry.

Viscosity losses, believed to be due to viscous heating, were observed at shear stresses greater than 10^4 N/m^2 (1.45 psi) for all test fluids (except the fluorinated polyether) at 38° C (100° F) and about 8×10^7 N/m^2 (1.2×10^4 psi).

---

*Professor of Mechanical Engineering, Georgia Institute of Technology, Atlanta, Georgia.

†Assistant Professor of Mechanical Engineering, Georgia Institute of Technology, Atlanta, Georgia.

INTRODUCTION

Advances in the field of thin film (e.g., elastohydrodynamic (EHD)) lubrication have dictated the need for information on the rheological behavior of lubricants under conditions of high temperature, high pressure, and high shear stress. A primary use of such information is for predicting the EHD film forming capability of high-temperature lubricants.

A number of investigators using a variety of techniques have reported pressure-viscosity data on lubricants. The most extensive study was carried out at Harvard University under the sponsorship of the ASME in 1953 (refs. 1 and 2). Pressure-viscosity data on more than forty fluids were reported using a falling weight viscometer developed by Bridgman (ref. 3) for pressures to 1.7×10^9 N/m^2 (2.5×10^5 psi). A similar type of viscometer capable of high pressures (2.7×10^9 N/m^2) (4×10^5 psi)) and high temperatures (218° C (425° F)) was also developed and reported by Bridgman (ref. 4). Wilson (ref. 5) also using a similar type of viscometer has measured viscosities at pressures to 1.2×10^9 N/m^2 (1.6×10^5 psi) for a number of lubricants. All of these viscometers are limited to low shear stresses (25 N/m^2 (3.6×10^{-3} psi)).

Philippoff (ref. 6), Appeldoorn, Okrent, and Philippoff (ref. 7), and more recently Rein, Charng, Sliepcovich, and Ewbank (ref. 8) have measured viscosities of lubricants at pressures to 2.75×10^8 N/m^2 (4×10^4 psi) using an oscillating crystal viscometer of the Mason type (ref. 9). Then, by using a reduced variable technique, viscosities obtained at discrete frequencies and at various pressures and temperatures can be converted to equivalent values at a single temperature and pressure and over a range of frequencies (i.e., shear rates). However, this type of viscometer has an upper viscosity limit of only about 1 N-sec/m^2 (1000 cP).

Foord, Hammann, and Cameron (ref. 10) and Westlake and Cameron (ref. 11) calculated effective pressure-viscosity coefficients for a variety of lubricants from film thickness data measured by optical elastohydrodynamics. This indirect method requires a standard fluid with known pressure-viscosity characteristics. A deficiency of this method is that the pressure and shear stress associated with the calculated pressure-viscosity coefficient must be estimated. However, this method does provide data for an actual condition of bearing operation.

Several investigators have utilized capillary viscometers for pressure-viscosity work. Some of the early workers using this type of viscometer were Hersey and Snyder (ref. 12), Norton, Knott, and Muenger (ref. 13), and, more recently, Klaus, Johnson, and Fresco (ref. 14). Capillary viscometers are capable of measurements at pressures to 6.9×10^8 N/m^2 (1×10^5 psi) with a wide range of viscosities (10^{-3} to 10^2 N-sec/m^2 (1.0 to 10^5 cP)) and shear stresses (30 to 7×10^6 N/m^2 (4.4×10^{-3} to 1×10^3 psi)) (refs. 15 and 16).

The objectives of this investigation were (1) to determine viscosities of a number of liquid lubricants and lubricant formulations as functions of pressure, temperature, and shear stress using a high-pressure capillary viscometer and (2) to compare, where possible, these results to those obtained by other techniques (optical elastohydrodynamics, oscillating crystal, and low shear capillary viscometry).

Conditions included a pressure range from atmospheric to 5.5×10^8 N/m^2 (8×10^4 psi) (in most cases), temperatures of 38°, 99°, and 149° C (100°, 210°, and 300° F), and shear stresses to 10^5 N/m^2 (14.5 psi). Tests were conducted at the Georgia Institute of Technology under NASA Contracts NAS3-14546 and NAS3-15383 and at the University of Michigan under NASA purchase order C-57357-B.

EXPERIMENTAL APPARATUS AND PROCEDURE

A high-pressure capillary viscometer has been constructed and reported in detail elsewhere (ref. 15). The viscometer is shown schematically in figure 1. The upper pressure limit of the device is 6.89×10^8 N/m^2 (1×10^5 psi) and the shear stress range is 30 to 5×10^6 N/m^2 (4.4×10^{-3} to 7×10^2 psi). The viscosity range is from somewhat less than 1×10^{-3} N-sec/m^2 (1 cP) to more than 100 N-sec/m^2 (10^5 cP). The temperature of the fluid sample is controlled by a constant temperature bath and can be varied from -46° to 232° C (-50° to 450° F).

Referring to figure 1 reveals that the test fluid is contained in reservoir R1 and R2 and in the high-pressure tubing connecting the two reservoirs to the test section which contains the capillary. The test section is immersed in the constant temperature bath. The fluid in the test section is pressurized by pumping low pressure hydraulic fluid into cavity I and venting cavity II. The high pressure is generated by an intensifier which has a 50 to 1 area ratio between piston P1 and the high-pressure piston P2. Flow through the capillary is caused by moving the translating piston along the two high-pressure rams. Movement along these rams is measured by a velocity transducer (TR4) which indicates the volumetric flow rate through the capillary. Care must be taken to ensure that no test fluid initially outside the constant temperature bath passes through the capillary during the time measurements are being made.

The test section consists of standard high-pressure tubing with stainless-steel capillary tubing pressed into it. The capillary tubing has a nominal inside diameter of 2.5×10^{-4} meter (0.01 in.). Several interchangeable capillaries of differing lengths were made so that a range of length-to-diameter ratios were available. This permits one to cover a wide range of shear rates and shear stresses with the instrument. The capillary diameters were determined in the usual manner of viscometry by calibration with viscosity standards.

The pressure level and pressure drop across the capillary were measured with commercial strain-gage pressure transducers indicated by TR1, TR2, and TR3, respectively, in figure 1. These were calibrated periodically with the two bourdon gages (B1, B2).

The electrical signals of TR2 and TR3 were nulled, through electrical balancing, at the pressure level of interest. Then by amplifying the signals from these transducers through high gain dc amplifiers, small fluctuations of pressure about the pressure level were detected with considerable accuracy.

The signals from the three pressure transducers and the velocity transducer were recorded continuously as a function of time. This enables one to use only steady-state behavior when deducing the viscosity of a fluid.

A detailed discussion of the calibration procedure, accuracy, and viscometric limitation of the apparatus have been published elsewhere (ref. 15).

DATA HANDLING

The standard techniques used in this study for interpreting data from capillary flows are fully described in references 17 and 18. The following assumptions were considered in this work:

(1) Time study flow

(2) Negligible entrance effects

(3) Negligible viscous heating

(4) Absence of thixotropic or rheopectic behavior

A brief description of the data handling procedure is given hereinafter. The shear stress at the capillary wall τ_w was determined from the following equation:

$$\tau_w = \frac{\Delta P}{4\left(\frac{L}{D}\right)} \tag{1}$$

where ΔP is the pressure differential across the capillary corrected for the kinetic energy of the fluid, L is the capillary length, and D is the capillary diameter. (Symbols are defined in appendix A.)

The apparent shear rate at the capillary wall for Newtonian fluids was determined from the following expression:

$$\dot{\gamma}_a = \frac{32Q}{\pi D^3} \tag{2}$$

where Q is the volumetric flow rate.

When non-Newtonian behavior is observed, the correct shear rate at the wall is determined by the Rabinowitsch technique (ref. 19) from

$$\dot{\gamma} = \frac{3 + S}{4} \dot{\gamma}_a \tag{3}$$

where

$$S = \frac{d \log \dot{\gamma}_a}{d \log \tau_w} \tag{4}$$

or the slope of the plot of $\log \dot{\gamma}_a$ as function of τ_w.

The fluid viscosity was then calculated from the corrected values of shear stress and and shear rate from

$$\mu = \frac{\tau_w}{\dot{\gamma}} \tag{5}$$

RESULTS AND DISCUSSION

Table I lists the thirteen lubricants and lubricant formulations studied in this investigation together with their atmospheric kinematic viscosities and densities.

Viscosity as a Function of Pressure

Absolute viscosity as a function of pressure for all test fluids appear in figure 2. The viscosity of each fluid is plotted as a function of pressure at three temperatures, 38°, 99°, and 149° C (100°, 210°, and 300° F). All data have been plotted on empirical rectifying charts developed by Roelands (ref. 20). A description of the Roelands format as well as other methods for correlating pressure-viscosity data appear in appendix B.

As is evident in figure 2 some nonlinear pressure-viscosity curves were obtained with a number of the test fluids. The nonlinearity was more pronounced at the higher temperatures. The Z parameter, which is the slope of the Roelands pressure-viscosity plots, was obtained by a least-squares fit to a straight line of the points used in the plotting routine. Table II contains Z values for all fluids at the three test temperatures. Roelands found that the Z value for any particular fluid is usually constant

over a wide temperature range. This is confirmed here with the only exceptions being the synthetic hydrocarbon (traction fluid) and the C-ether.

Atmospheric pressure-viscosity coefficients α_{0_T} have been determined for all test fluids and appear in table III. Reciprocal asymptotic isoviscous pressure α^* for all fluids appear in table IV. Values of α^* as a function of temperature appear in figure 3. The order of α^* values for the unformulated fluids at 38° C (100° F) are: fluorinated polyether > synthetic hydrocarbon (traction fluid) > super-refined naphthenic mineral oil > synthetic paraffinic oil (lot 4) > C-ether ≅ synthetic paraffinic oil (lot 3) > polyalkyl aromatic > advanced ester.

Elastohydrodynamic Film Forming Capability

A convenient parameter for rating the EHD film forming ability of a group of fluids is the product of the reciprocal asymptotic isoviscous pressure α^* and the atmospheric absolute viscosity μ_0. Values of this parameter $\alpha^*\mu_0$ are tabulated for all fluids at the three test temperatures in table V. In addition, $\alpha^*\mu_0$ as a function of temperature for the unformulated fluids appears in figure 4. At 38° C (100° F) the order of the EHD film forming ability of the unformulated fluids is as follows: fluorinated polyether ≅ synthetic paraffinic oil (lot 4) ≅ synthetic paraffinic oil (lot 3) > super-refined naphthenic mineral oil > synthetic hydrocarbon (traction fluid) > C-ether > polyalkyl aromatic > advanced ester. As is evident in figure 4, some reordering may occur at higher temperatures.

Effect of Structure on Pressure-Viscosity

Based on structural considerations, one would qualitatively predict the following order of pressure-viscosity coefficients for the different fluid classes: highly halogenated fluids > rigid naphthenes (cycloalkanes) > rigid aromatics > fluids composed of flexible straight chain molecules (refs. 20 to 23). Of course, the fluids in this study are not so easily classified. For example, traction fluids are usually a blend of a cycloalkane and a straight chain fluid. Mineral oils are complex mixtures of naphthenes and isoparaffins. Synthetic paraffinic oils are essentially ring free but may contain some chain branching. C-ethers contain several aromatic isomers but also have a flexible sulfur linkage between the rings. Polyalkyl aromatics may behave like aromatics or paraffins depending on the length of the alkyl side-chains. In addition, there are chain length or molecular weight effects in some fluid classes. Therefore, at 38° C (100° F) the α^* values for the unformulated test fluids essentially follow the predicted order if the aforementioned considerations are taken into account.

Fluids that have high viscosity-pressure indices Z also have steep viscosity temperature slopes. Therefore, their α^* values decrease more rapidly with increasing temperature than low Z fluids. This behavior, which is illustrated in figure 3 can cause a reordering of the α^* values at the higher temperatures.

Effect of Additives on Pressure-Viscosity

Five formulated fluids were included in this study. They were: (1) formulated advanced ester, (2) super-refined naphthenic mineral oil plus 5 weight percent heavy resin, (3) polyalkyl aromatic plus 10 weight percent heavy resin, (4) synthetic paraffinic oil (lot 2) plus an antiwear additive, and (5) the synthetic paraffinic oil (lot 4) plus an antiwear additive.

Viscosity-pressure curves for the aforementioned formulations and their base fluids appear in figure 2. Values of α_{0T} and α^* for all fluids appear in tables III and IV, respectively. Figure 3 shows α^* plotted against temperature. Values of $\alpha^*\mu_0$ values appear in table V.

In general, the ester, mineral oil, and aromatic formulations exhibited higher viscosities than their respective base fluids over the entire pressure range. This was to be expected with the high molecular weight heavy resin additive in the mineral oil and aromatic formulations. Figures 2(d) and (e) contain viscosity-pressure curves for a synthetic paraffinic oil with and without an antiwear additive. Four different fluids (two base fluids and two formulations) from three different lots were tested. The different pressure-viscosity characteristics noted in figure 2(d) result from the fact that lots 2 and 3 had different base viscosities. However, both fluids shown in figure 2(e) are from the same lot. A small amount of an organic phosphonate antiwear additive has been added to the base fluid. A large viscosity change would not be expected from such an additive and, indeed, only small reductions in viscosity are noted.

In general, the additives in the aforementioned formulations were added to improve boundary lubricating characteristics of the base fluids. However, the organic phosphonate antiwear additive has yielded some surprising results in EHD film thickness and traction measurements. Parker and Kannel (ref. 24) reported that this phosphonate additive caused an increase of 50×10^{-8} to 100×10^{-8} meters (20 to 40 μin.) in the EHD film thickness when compared to the base fluid (from the same lot) results under identical conditions. It was speculated that this phenomenon was due to a change in fluid rheology caused by a chemically adsorbed surface film. Recently, Trachman and Cheng (ref. 25) reported traction data for the synthetic paraffinic oil (lot 4) with and without the phosphonate additive. Consistently lower traction coefficients were obtained for the additive fluid when compared to the base fluid under identical conditions. Again, it was

theorized that an increase in film thickness for the formulated fluid compared to the base fluid would explain the traction results.

Small increases in α^* and $\alpha^*\mu_0$ were observed for the formulated advanced ester, the polyalkyl aromatic plus 10 weight percent heavy resin, and the super-refined naphthenic mineral oil plus 5 weight percent heavy resin as compared to their respective base fluids. Essentially, no difference was noted for the synthetic paraffinic oil plus an antiwear additive (lot 4) when compared to its base fluid. Therefore, one would expect slightly thicker EHD films to be generated with the ester and heavy resin formulations but no increase for the synthetic paraffinic formulation. Preliminary film thickness measurements by optical elastohydrodynamics confirm this expectation.

Comparison of Pressure-Viscosity Results with Reference Data

Some of the test fluids included in this program have been studied by other investigators. Foord, Hammann, and Cameron (ref. 10) and Westlake and Cameron (ref. 11) utilized optical electrohydrodynamics to determine effective α values. Rein, Charng, Sliepcovich, and Ewbank (ref. 8) used an oscillating crystal apparatus and Fresco (ref. 26) a low shear capillary viscometer.

Table VI contains a comparison of α values for the common fluids. Comparisons are made at 38° C (100° F) and 6.9×10^7 N/m^2 (1×10^4 psi), where possible. The optical EHD data were taken at room temperature and the pressure associated with the α values is only approximate.

Two factors must be considered when making comparisons in table VI. If the optical data (refs. 10 and 11) had been taken at 38° C (100° F), slightly lower α values would have resulted (α decreases with increasing temperature). Also, the capillary data from this study and that of Fresco (ref. 26), shown in table VI, were taken at shear rates well below any threshold for non-Newtonian behavior. Both the optical and oscillating crystal data were taken at shear rates where shear thinning may occur. The optical EHD results may also be subject to viscous heating due to the high shear rate in the inlet. Both of these effects would result in lower viscosities and thus lower calculated α values.

Table VII contains the shear stress levels associated with the values from table VI. In general, the α values decrease with increasing shear stress. In light of the previous discussion, there appears to be fair agreement among the various investigators and their different techniques.

Rein, Charng, Sliepcovich, and Ewbank (ref. 8) studied four common fluids at temperatures of 38°, 99°, and 149° C (100°, 210°, and 300° F) and pressures to 2.7×10^8 N/m^2 (4×10^4 psi). These viscosity-pressure curves appear in figure 5 with the capillary data for comparison. As mentioned previously, Rein's data were taken at high effective

shear stresses (usually $>10^5$ N/m^2 (14.5 psi)). Therefore, lower viscosities for the oscillating crystal data might be expected and, in general, this is the case.

Viscosity as a Function of Shear Stress

Viscosity as a function of shear stress at 38° C (100° F) and constant pressure (approximately 8.3×10^7 N/m^2 (1.2×10^4 psi)) for all fluids appear in figure 6. All fluids, except the fluorinated polyether, exhibited viscosity losses in the shear stress range 10^4 to 10^5 N/m^2 (1.45 and 14.5 psi). This behavior is believed to be due to viscous heating. Calculations indicate that the pressure drop across the capillary for many of the experiments in this study at high shear stress values was large enough ($>3.5\times10^6$ N/m^2 (>500 psi)) to cause appreciable viscous heating. A detailed study of capillary heating effects and high shear stress behavior of lubricants has recently been reported (ref. 27).

Comparison of Capillary Data with Oscillatory Data

The data of Rein (ref. 8) for the synthetic paraffinic oil and the reduced variable technique of Philippoff (refs. 6 and 7) were used to construct a plot of reduced viscosity μ_r against reduced angular frequency ω_r (i.e., shear rate). This curve appears in figure 7 along with the unreduced capillary data of figure 6. In order to make this comparison, the angular frequency ω in oscillatory shear is assumed equal to the shear rate γ in continuous shear. This assumption, of course, is very questionable but should be adequate for qualitative comparison. Although there is a great deal of scatter in the reduced data, the oscillatory results have been represented by a straight line at about 1 N-sec/m^2 (10^3 cP). It should be noted that, if a viscosity decrease were observed for the oscillatory data, a non-Newtonian (viscoelastic) mechanism would be indicated. Since the viscosity decrease observed with the capillary data has been ascribed to viscous heating, a correlation would not be expected.

SUMMARY OF RESULTS

A high-pressure capillary viscometer was used to measure viscosity as a function of pressure, temperature, and shear stress for a number of liquid lubricants. Measurements were made at 38°, 99°, and 149° C (100°, 210°, and 300° F), gage pressures to 5.5×10^8 N/m^2 (8×10^4 psi), and shear stresses to 10^5 N/m^2 (14.5 psi). The major results were:

1. At 38° C (100° F) the order of the pressure viscosity coefficients expressed as the reciprocal asymptotic isoviscous pressure α^* for the unformulated fluids was

fluorinated polyether > synthetic hydrocarbon (traction fluid) > super-refined naphthenic mineral oil > synthetic paraffinic oil (lot 4) > C-ether ≅ synthetic paraffinic oil (lot 3) > polyalkyl aromatic > advanced ester. All α^* values decreased with increasing temperature.

2. At 38° C (100° F) the order of the electrohydrodynamic (EHD) film forming capability $\alpha^*\mu_0$ was fluorinated polyether ≅ synthetic paraffinic oil (lot 4) ≅ synthetic paraffinic oil (lot 3) > super-refined naphthenic mineral oil > synthetic hydrocarbon (traction fluid) > C-ether > polyalkyl aromatic > advanced ester.

3. Small increases in α^* and $\alpha^*\mu_0$ were observed for the formulated advanced ester, the polyalkyl aromatic plus 10 weight percent heavy resin, and the super-refined naphthenic mineral oil plus 5 weight percent heavy resin as compared to their respective base fluids. Essentially, no difference was noted for the synthetic paraffinic oil (lot 4) plus an antiwear additive as compared to its base fluid.

4. Fair agreement was obtained when pressure-viscosity coefficients at 38° C (100° F) and 6.9×10^7 N/m^2 (10^4 psi) were compared to data from other investigators using different techniques.

5. Viscosity losses, believed to be due to viscous heating, were observed with increasing stresses at stresses greater than 10^4 N/m^2 (1.45 psi) for all test fluids (except the fluorinated polyether) at 38° C (100° F) and about 8×10^7 N/m^2 (1.2×10^4 psi).

Lewis Research Center,
National Aeronautics and Space Administration,
Cleveland, Ohio, May 9, 1974,
501-24.

APPENDIX A

SYMBOLS

D	capillary diameter, m
H	viscosity function, $\log (\log \mu_P + 1.200)$
H_0	viscosity function, $\log (\log \mu_0 + 1.200)$
L	capillary length, m
P	gage pressure, N/m^2
ΔP	pressure differential across capillary, N/m^2
S	slope of $\log \dot{\gamma}_a$ as a function of τ_w
Q	volumetric flow rate, m^3/sec
Z	viscosity-pressure index, dimensionless
α	pressure-viscosity coefficient from Barus equation, $(N/m^2)^{-1}$
α^*	reciprocal asymptotic isoviscous pressure, $\left[\int_0^\infty \frac{\mu_0 \, dP}{\mu_P}\right]^{-1}$, $(N/m^2)^{-1}$
α_{0T}	slope of the tangent to $\log \mu$ as a function of P isotherm at atmospheric pressure, $(N/m^2)^{-1}$
γ	shear rate, sec^{-1}
$\dot{\gamma}$	corrected shear rate at capillary wall, sec^{-1}
$\dot{\gamma}_a$	apparent shear rate at capillary wall, sec^{-1}
μ	absolute viscosity, $N\text{-}sec/m^2$
μ_P	absolute viscosity at pressure P, $N\text{-}sec/m^2$
μ_r	reduced absolute viscosity, $N\text{-}sec/m^2$
μ_0	absolute viscosity at atmospheric pressure, $N\text{-}sec/m^2$
ν	kinematic viscosity, m^2/sec
π	pressure function, $\log\left(1 + \frac{P}{2000}\right)$
ρ	density, kg/m^3
τ_w	wall shear stress, N/m^2

ω angular frequency, rad/sec

ω_r reduced angular frequency, rad/sec

APPENDIX B

PRESSURE-VISCOSITY PARAMETERS

The most extensively used empirical pressure-viscosity correlation is that developed by Barus (ref. 28):

$$\mu_P = \mu_0 e^{\alpha P} \tag{B1}$$

where μ_P is the absolute viscosity at gage pressure P, μ_0 is the absolute viscosity at atmospheric pressure, and α is a constant which is temperature dependent but pressure independent. Therefore, a plot of log μ as a function of P would appear as a straight line having a slope of α and an atmospheric pressure intercept of μ_0. Unfortunately, pressure-viscosity data seldom follow this simple relation, except in the very low pressure range. A typical pressure-viscosity isotherm which illustrates this point appears in figure 8.

The slope of the tangent to the log μ as function of P isotherm at atmospheric pressure (designated as α_{0T} in fig. 8) is often used in EHD analysis and film thickness calculations. Others have used the slope of the secant obtained by passing a line through the log μ as function of P isotherm at atmospheric and 7×10^7-N/m^2 (10^4-psi) pressures (designated α_{0S10K} in fig. 8).

Roelands (ref. 20) has developed a new correlational method for pressure-viscosity data based on the following empirical equation:

$$\log \mu + 1.200 = (\log \mu_0 + 1.200)\left(1 + \frac{P}{2000}\right)^Z \tag{B2}$$

where μ is the absolute viscosity in centipoise, P is the gage pressure in kgf/cm^2, and and μ_0 is the absolute viscosity in centipoise at atmospheric pressure and at the same temperature. Equation (B2) can be rewritten in the following form:

$$H = Z\pi + H_0 \tag{B3}$$

where H is the viscosity function log (log μ_P + 1.200), π is the pressure function log[1 + (P/2000)] and H_0 is log (log μ_0 + 1.200). By constructing scales proportional to H and π a rectifying chart is obtained. The scales are so proportioned that the upward slope of the pressure-viscosity lines is numerically equal to the viscosity-pressure index Z. The use of these charts has been reported to rectify (linearize) all pressure-viscosity data.

Roelands (ref. 20) and Blok (ref. 29) also advocate the use of another pressure-viscosity parameter, the reciprocal asymptotic isoviscous pressure α^* (which is obtained from a Weibull transformation). The definition of α^* is shown in figure 8. The parameter α^* takes into account all variations of viscosity with pressure over the entire pressure range and is probably the least dependent of all the parameters on measurement techniques.

The relation between α_{0T} and Z is as follows:

$$\log \alpha_{0T} = \log Z + H_0 - 2.9388 \tag{B4}$$

No simple relation exists between α^* and Z. However, Roelands (ref. 20) does provide a table showing α^* as a function of Z and H_0.

REFERENCES

1. ASME Pressure Viscosity Report, Vol. 1. ASME, New York, 1953.
2. ASME Pressure Viscosity Report, Vol. II. ASME, New York, 1953.
3. Bridgman, P. W.: Effect of Pressure on the Viscosity of 43 Pure Liquids. Proc. Am. Acad. Arts Sci., vol. 61, 1926, pp. 57-91.
4. Bridgman, P. W.: Viscosities to 30,000 kg/cm^2. Proc. Amer. Acad. Arts Sci., vol. 77, no. 4, Feb. 1949, pp. 115-128.
5. Wilson, D. R.: Exploratory Development on Advanced Fluids and Lubricants in Extreme Environments by Mechanical Characterization. Midwest Research Institute (AFML-TR-70-32-Pt. 3; AD-891509L), 1972.
6. Philippoff, W.: Viscoelasticity of Polymer Solutions at High Pressures and Ultrasonic Frequencies. J. Appl. Phys., vol. 34, no. 5, May 1963, pp. 1507-1511.
7. Appeldoorn, J. K.; Okrent, E. H.; and Philippoff, W.: Viscosity and Elasticity at High Pressures and High Shear Rates. Proc. Amer. Pet. Inst., vol. 42, no. 3, 1962, pp. 163-172.
8. Rein, R. G.; Charng, T. T.; Sliepcovich, C. M.; and Ewbank, W. J.: Measurement of the Viscosity by Oscillating Crystal Method of Four Fluids as Functions of Pressure, Shear Rate, and Temperature. ER-1754-1, Univ. of Okla. Res. Inst. (NASA CR-120786), 1971.
9. Mason, W. P.: Measurement of the Viscosity and Shear Elasticity of Liquids by Means of a Torsionally Vibrating Crystal. Trans. ASME, vol. 69, May 1947, pp. 359-370.
10. Foord, C. A.; Hammann, W. C.; and Cameron, A.: Evaluation of Lubricants Using Optical Elastohydrodynamics. ASLE Trans., vol. 11, no. 1, Jan. 1968, pp. 31-43.
11. Westlake, F. J.; and Cameron, A.: Optical Elastohydrodynamic Fluid Testing. ASLE Trans., vol. 15, no. 2, April 1972, pp. 81-95.
12. Hersey, M. D.; and Snyder, G. H.: High Pressure Capillary Flow. J. Rheology, vol. 3, no. 3, Jul. 1932, pp. 298-317.
13. Norton, A. E.; Knott, M. J.; and Muenger, J. R.: Flow Properties of Lubricants under High Pressure. Trans. ASME, vol. 63, Oct. 1941, pp. 631-643.
14. Klaus, E. F.; Johnson, R. H.; and Fresco, G. P.: Development of a Precision Capillary-Type Pressure Viscometer. ASLE Trans., vol. 9, no. 2, April 1966, pp. 113-120.

15. Novak, J. D.; and Winer, W. O.: Some Measurements of High Pressure Lubricant Rheology. J. Lubr. Tech., vol. 90, no. 3, July 1968, pp. 580-591.

16. Carlson, S.; Turchina, V.; Jakobsen, J.; Sanborn, D. M.; and Winer, W. O.: Investigations of Lubricant Rheology as Applied to Elastohydrodynamic Lubrication. Georgia Institute of Technology (NASA CR-134539), 1974.

17. Philippoff, W.; and Gaskins, F. H.: The Capillary Experiment in Rheology. Trans. Soc. Rheology, vol. 11, 1958, pp. 263-284.

18. Van Wazer, John R., et al.: Viscosity and Flow Measurement. Interscience Publications, 1963.

19. Rabinowitsch, B.: Ubër Die Viskositat und Elastisitat Von Solen. Zeit. fur Physik. Chemie, Abt. A., Bd. 145, Heft. 1, 1929.

20. Roelands, C. H. A.: Correlational Aspects of the Viscosity-Temperature-Pressure Relationship of Lubricating Oils. O. P. Books Program, University Microfilm, Ann Arbor, Michigan, 1966.

21. Lowitz, D. A.; Spencer, J. W.; Webb, W.; and Schiessler, R. W.: Temperature-Pressure-Structure Effects on the Viscosity of Several Higher Hydrocarbons. J. Chem. Phys., vol. 30, no. 1, Jan. 1959, pp. 73-83.

22. Bondi, A.: Viscosity and Molecular Structure. In Rheology, Vol. 4. F. R. Eirich, ed., Academic Press, 1967, pp. 1-83.

23. Kuss, E.: Extreme Values of the Pressure Coefficient of Viscosity. Angew. Chem. Internat. Edit., vol. 4, no. 11, 1965, pp. 944-950.

24. Parker, Richard J.; and Kannel, Jerrold W.: Elastohydrodynamic Film Thickness between Rolling Disks with a Synthetic Paraffinic Oil to 589 K (600° F). NASA TN D-6411, 1971.

25. Trachman, E. G.; and Cheng, H. S.: Traction in Elastohydrodynamic Line Contacts for Two Synthesized Hydrocarbon Fluids. Preprint 73-LC-4A-1, ASLE, Oct. 1973.

26. Fresco, G. P.: Measurement and Prediction of Viscosity-Pressure Characteristics of Liquids. M.S. Thesis, Penn. State Univ., 1966.

27. Jakobsen, J.: Lubricant Rheology at High Shear Stress. Ph.D. Thesis, Georgia Institute of Technology, 1973.

28. Barus, C.: Isothermals, Isopiestics and Isometrics Relative to Viscosity. Am. J. Sci., vol. 45, 1893, pp. 87-96.

29. Blok, H.: Inverse Hydrodynamics. Proceedings of the International Symposium on Lubrication and Wear. D. Muster and B. Steinlicht, eds., McCutchan Publ. Corp., Berkeley, Calif., 1964, pp. 1-151.

TABLE I. - KINEMATIC VISCOSITIES AND DENSITIES OF TEST FLUIDS AT ATMOSPHERIC PRESSURE AND THREE TEMPERATURES

(a) SI units

Test fluids	Kinematic viscosity, ν, m^2/sec	Density, ρ, kg/m^3	Kinematic viscosity, ν, m^2/sec	Density, ρ, kg/m^3	Kinematic viscosity, ν, m^2/sec	Density, ρ, kg/m^3
	38° C		99° C		149° C	
Advanced ester	2.58×10^{-5}	979	0.51×10^{-5}	932	0.23×10^{-5}	895
Formulated advanced ester	2.82	980	.53	935	.24	897
Polyalkyl aromatic	3.0	851	.50	815	.23	783
Polyalkyl aromatic + 10 wt.% heavy resin	3.77	853	.61	814	.26	781
Synthetic paraffinic oil (lot 3)	49.3	839	4.26	806	1.4	778
Synthetic paraffinic oil (lot 4)	44.7	839	4.04	806	1.3	778
Synthetic paraffinic oil (lot 4) + anti-wear additive	44.7	839	4.04	806	1.3	778
Synthetic paraffinic oil (lot 2) + anti-wear additive	44.2	836	4.0	799	1.29	770
C-ether	2.5	1180	.41	1140	.20	1100
Super-refined naphthenic mineral oil	7.8	873	.82	836	.33	803
Super-refined naphthenic mineral oil + 5 wt.% heavy resin	9.19	876	.94	838	.35	805
Synthetic hydrocarbon (traction fluid)	3.72	922	.40	882	.19	850
Fluorinated polyether	9.66	1870	1.15	1760	.4	1670

TABLE I. - Concluded. KINEMATIC VISCOSITIES AND DENSITIES OF TEST FLUIDS AT ATMOSPHERIC PRESSURE AND THREE TEMPERATURES

(b) U. S. Customary units

Test fluids	Kinematic viscosity, ν, cS	Density, ρ, g/ml	Kinematic viscosity, ν, cS	Density, ρ, g/ml	Kinematic viscosity, ν, cS	Density, ρ, g/ml
	100° F		210° F		300° F	
Advanced ester	25.8	0.979	5.1	0.932	2.3	0.895
Formulated advanced ester	28.2	.980	5.3	.935	2.4	.897
Polyalkyl aromatic	30.0	.851	5.0	.815	2.3	.783
Polyalkyl aromatic + 10 wt.% heavy resin	37.7	.853	6.1	.814	2.6	.781
Synthetic paraffinic oil (lot 3)	493	.839	42.6	.806	14.0	.778
Synthetic paraffinic oil (lot 4)	447	.839	40.4	.806	13.0	.778
Synthetic paraffinic oil (lot 4) + anti-wear additive	447	.839	40.4	.806	13.0	.778
Synthetic paraffinic oil (lot 2) + anti-wear additive	442	.836	40.0	.799	12.9	.770
C-ether	25.0	1.18	4.1	1.14	2.0	1.10
Super-refined naphthenic mineral oil	78.0	.873	8.2	.836	3.3	.803
Super-refined naphthenic mineral oil + 5 wt.% heavy resin	91.9	.876	9.4	.838	3.5	.805
Synthetic hydrocarbon (traction fluid)	37.2	.922	4.0	.882	1.9	.850
Fluorinated polyether	96.6	1.87	11.5	1.76	4.0	1.67

TABLE II. - PRESSURE-VISCOSITY INDEX FOR TEST FLUIDS

AT THREE TEMPERATURES

Test fluids	Pressure-viscosity index, Z, dimensionless		
	38° C (100° F)	99° C (210° F)	149° C (300° F)
Advanced ester	0.48	0.48	0.48
Formulated advanced ester	.49	.47	.49
Polyalkyl aromatic	.55	.54	.55
Polyalkyl aromatic + 10 wt. % heavy resin	.55	.55	.56
Synthetic paraffinic oil (lot 3)	.43	.44	.39
Synthetic paraffinic oil (lot 4)	.44	.46	.47
Synthetic paraffinic oil (lot 4) + anti-wear additive	.44	.46	.46
Synthetic paraffinic oil (lot 2) + anti-wear additive	.43	.44	.43
C-ether	.72	.50	.50
Super-refined naphthenic mineral oil	.67	.67	.64
Super-refined naphthenic mineral oil + 5 wt. % heavy resin	.68	.65	.66
Synthetic hydrocarbon (traction fluid)	1.06	.85	.69
Fluorinated polyether	.77	.79	.80

TABLE III. - ATMOSPHERIC PRESSURE-VISCOSITY COEFFICIENTS FOR TEST FLUIDS AT THREE TEMPERATURES

Test fluids	Atmospheric pressure-viscosity coefficient, α_{0T}					
	$(N/m^2)^{-1}$	psi^{-1}	$(N/m^2)^{-1}$	psi^{-1}	$(N/m^2)^{-1}$	psi^{-1}
	38° C (100° F)		99° C (210° F)		149° C (300° F)	
Advanced ester	1.52×10^{-8}	1.05×10^{-4}	1.38×10^{-8}	0.95×10^{-4}	1.34×10^{-8}	0.92×10^{-4}
Formulated advanced ester	1.84	1.27	1.48	1.02	1.22	.84
Polyalkyl aromatic	2.03	1.40	1.74	1.20	1.45	1.00
Polyalkyl aromatic + 10 wt. % heavy resin	2.06	1.42	1.81	1.25	1.50	1.03
Synthetic paraffinic oil (lot 3)	2.03	1.40	2.22	1.53	1.41	.97
Synthetic paraffinic oil (lot 4)	2.84	1.96	2.69	1.85	2.55	1.76
Synthetic paraffinic oil (lot 4) + anti-wear additive	2.84	1.96	2.69	1.85	2.55	1.76
Synthetic paraffinic oil (lot 2) + anti-wear additive	2.03	1.40	1.81	1.25	1.48	1.02
C-ether	1.45	1.00	.91	.63	.74	.51
Super-refined naphthenic mineral oil	3.08	2.12	1.81	1.25	1.34	.92
Super-refined naphthenic mineral oil + 5 wt. % heavy resin	2.67	1.84	2.15	1.48	1.81	1.25
Synthetic hydrocarbon (traction fluid)	3.15	2.17	1.36	.94	1.50	1.03
Fluorinated polyether	4.46	3.07	4.38	3.02	4.35	3.00

TABLE IV. - PRESSURE-VISCOSITY COEFFICIENTS FOR TEST FLUIDS EXPRESSED AS RECIPROCAL ASYMPTOTIC ISOVISCOUS PRESSURES AT THREE TEMPERATURES

Test fluids	Reciprocal asymptotic isoviscous pressure, α^*					
	$(N/m^2)^{-1}$	psi^{-1}	$(N/m^2)^{-1}$	psi^{-1}	$(N/m^2)^{-1}$	psi^{-1}
	38° C (100° F)		99° C (210° F)		149° C (300° F)	
Advanced ester	1.28×10^{-8}	0.885×10^{-4}	0.987×10^{-8}	0.680×10^{-4}	0.851×10^{-8}	0.586×10^{-4}
Formulated advanced ester	1.37	.942	1.00	.691	.874	.602
Polyalkyl aromatic	1.58	1.09	1.25	.862	1.01	.697
Polyalkyl aromatic + 10 wt.% heavy resin	1.70	1.17	1.28	.885	1.06	.729
Synthetic paraffinic oil (lot 3)	1.77	1.22	1.51	1.04	1.09	.750
Synthetic paraffinic oil (lot 4)	1.99	1.37	1.51	1.04	1.29	.890
Synthetic paraffinic oil (lot 4) + anti-wear additive	1.96	1.35	1.55	1.07	1.25	.860
Synthetic paraffinic oil (lot 2) + anti-wear additive	1.81	1.25	1.37	.941	1.13	.782
C-ether	1.80	1.24	.980	.675	.795	.548
Super-refined naphthenic mineral oil	2.51	1.73	1.54	1.06	1.27	.873
Super-refined naphthenic mineral oil + 5 wt.% heavy resin	2.51	1.73	1.74	1.20	1.37	.941
Synthetic hydrocarbon (traction fluid)	3.12	2.15	1.71	1.18	.939	.647
Fluorinated polyether	4.17	2.87	3.24	2.23	3.02	2.08

TABLE V. - ELASTOHYDRODYNAMIC FILM FORMING

CAPABILITY OF TEST FLUIDS

Test fluids	$\alpha^* \mu_0$, sec		
	38° C (100° F)	99° C (210° F)	149° C (300° F)
Advanced ester	32.2×10^{-11}	4.6×10^{-11}	1.8×10^{-11}
Formulated advanced ester	37.8	5.0	1.9
Polyalkyl aromatic	40.3	5.1	1.8
Polyalkyl aromatic + 10 wt. % heavy resin	54.7	6.4	2.2
Synthetic paraffinic oil (lot 3)	733	51.8	11.9
Synthetic paraffinic oil (lot 4)	748	47.7	13.2
Synthetic paraffinic oil (lot 4) + anti-wear additive	737	49.0	12.8
Synthetic paraffinic oil (lot 2) + anti-wear additive	668	43.7	11.2
C-ether	53.3	4.6	1.7
Super-refined naphthenic mineral oil	171	10.5	3.4
Super-refined naphthenic mineral oil + 5 wt. % heavy resin	202	13.7	3.9
Synthetic hydrocarbon (traction fluid)	107	6.0	1.5
Fluorinated polyether	751	65.4	20.2

TABLE VI. - COMPARISON OF PRESSURE-VISCOSITY COEFFICIENTS WITH REFERENCE DATA

Test fluids	Pressure-viscosity coefficients									
	$(N/m^2)^{-1}$	psi^{-1}	$(N/m^2)^{-1}$	psi^{-1}	$(N/m^2)^{-1}$	psi^{-1}	$(N/m^2)^{-1}$	psi^{-1}	$(N/m^2)^{-1}$	psi^{-1}
	α^*		Reference data, α_{0S10K}							
	Capillary data 38° C (100° F)		Optical EHD (ref. 10) ~24° C (75° F)		Optical EHD (ref. 11) ~22° C (71° F)		Ultrasonic (ref. 8) 38° C (100° F)		Capillary (ref. 26) 38° C (100° F)	
Super-refined naphthenic mineral oil	2.51×10^{-8}	1.73×10^{-4}	2.15×10^{-8}	1.48×10^{-4}	---	---	2.15×10^{-8}	1.48×10^{-4}	2.47×10^{-8}	1.70×10^{-4}
Super-refined naphthenic mineral oil + 5 wt.% heavy resin	2.51	1.73	2.05	[a]1.41	---	---	---	---	---	---
Super-refined naphthenic mineral oil + 10 wt.% heavy resin	---	---	1.77	[b]1.22	---	---	2.25	1.55	---	---
Synthetic paraffinic oil (lot 3)	1.77	1.22	1.34	.92	1.81×10^{-8}	1.25	1.39	.96	---	---
Synthetic paraffinic oil (lot 2) + anti-wear additive	1.81	1.25	1.34	.92	---	---	---	---	---	---
C-ether	1.80	1.24	1.81	1.25	---	---	---	---	---	---
Fluorinated polyether	4.17	2.87	3.63	[c]2.50	3.69	2.54	3.02	2.08	---	---

[a]Unpublished data (5.5 wt.% heavy resin).

[b]Unpublished data (8.75 wt.% heavy resin).

[c]Corrected value; original data from ref. 10 was in error.

TABLE VII. - SHEAR STRESS LEVELS ASSOCIATED WITH PRESSURE-VISCOSITY COEFFICIENTS IN TABLE VI

Test fluids	Shear stress at 6.9×10^7 N/m^2 (10^4 psi), N/m^2				
	Capillary data 38° C (100° F)	Reference data			
		Optical EHD (ref. 10) ~24° C (75° F)	Optical EHD (ref. 11) ~22° C (71° F)	Ultrasonic (ref. 8) 38° C (100° F)	Capillary (ref. 26) 38° C (100° F)
Super-refined naphthenic mineral oil	$<0.1\times10^5$	7.0×10^5	---	1 to 2×10^5	$<<0.1\times10^5$
Super-refined naphthenic mineral oil + 5 wt. % heavy resin	<.1	[a]6.6	---	---	---
Super-refined naphthenic mineral oil + 10 wt. % heavy resin	---	[b]6.5	---	1.0	---
Synthetic paraffinic oil (lot 3)	<.1	5.5	(c)	1 to 4	---
Synthetic paraffinic oil (lot 2) + anti-wear additive	<.1	5.5	---	---	---
C-ether	<.1	6.3	---	---	---
Fluorinated polyether	<.1	11	1.1	4.0	---

[a]Unpublished data (5.5 wt. % heavy resin).
[b]Unpublished data (8.75 wt. % heavy resin).
[c]No value reported.

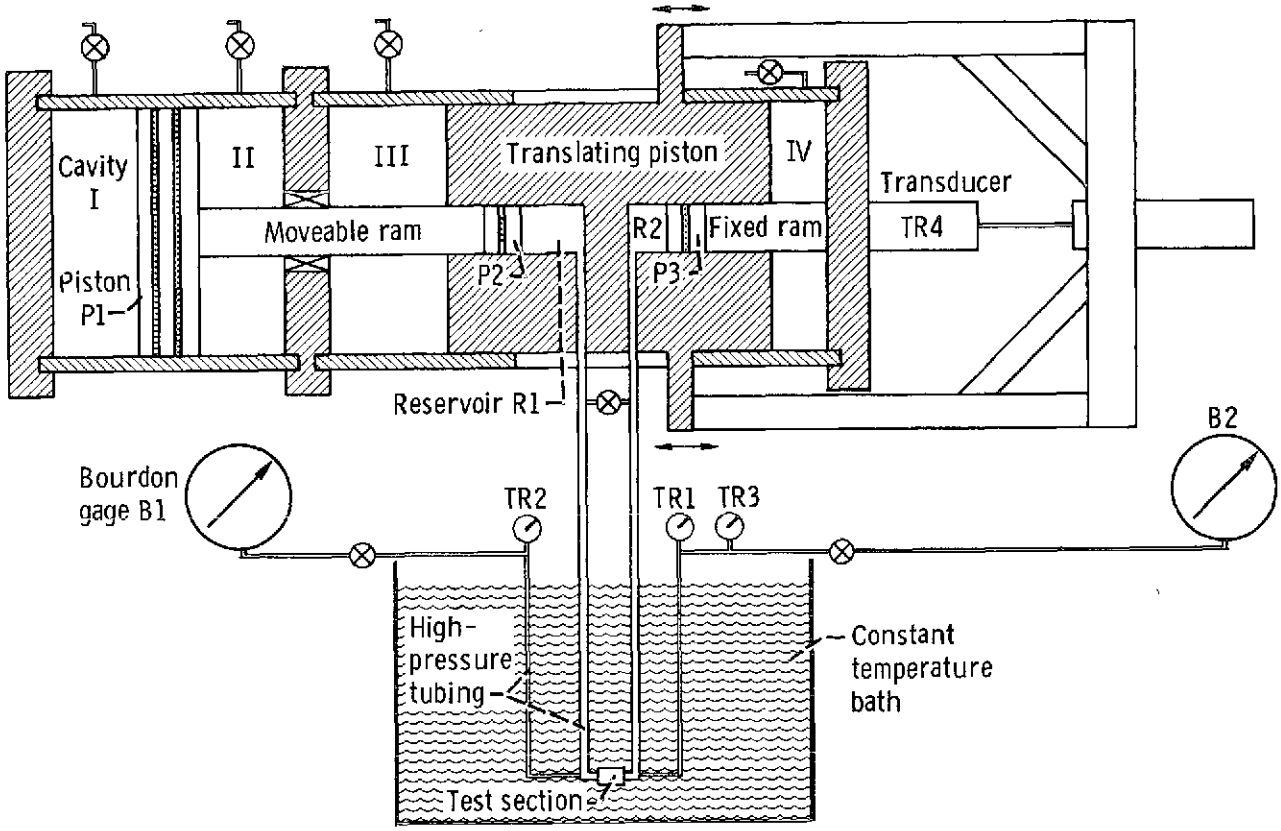

Figure 1. - Schematic of high-pressure capillary viscometer.

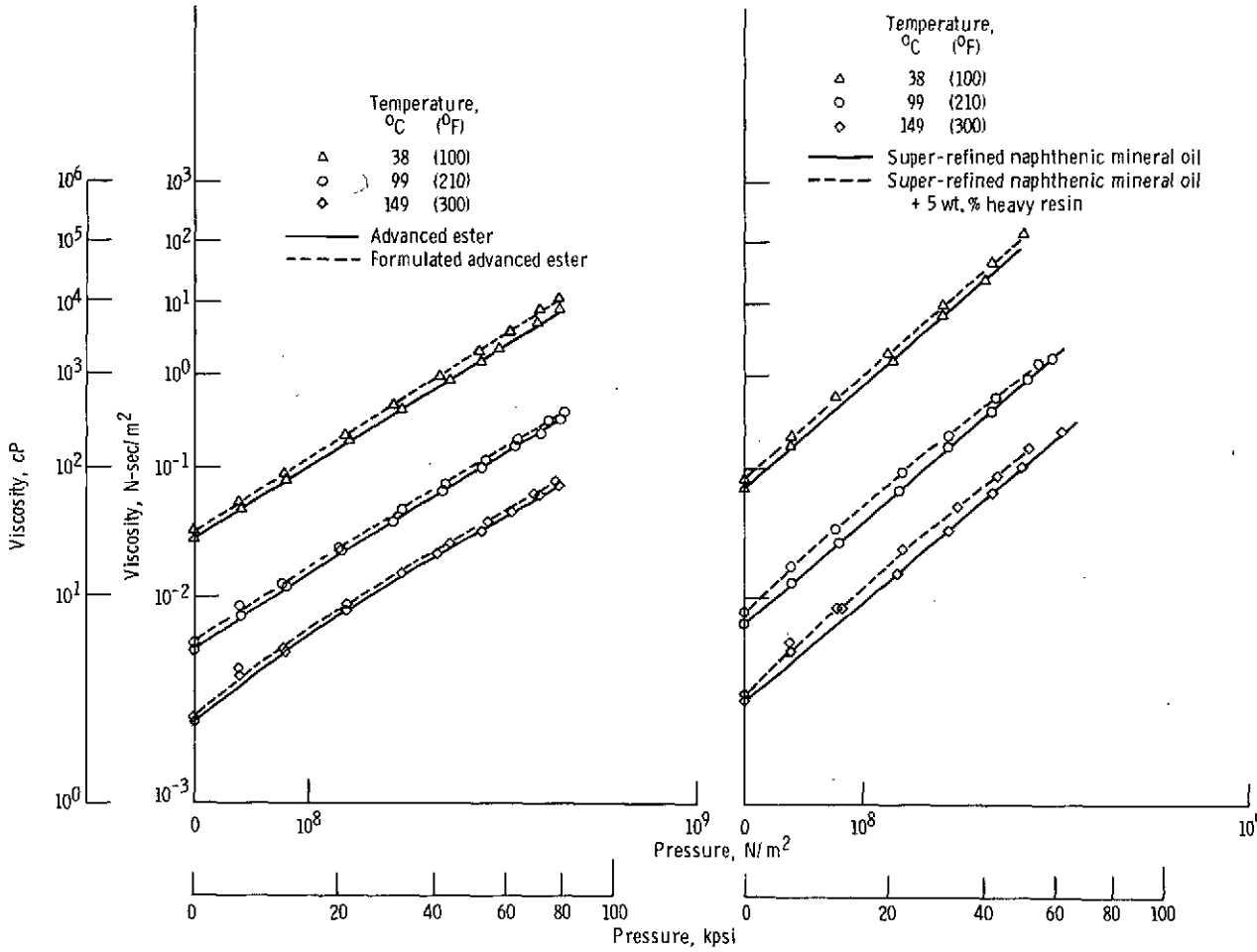

(a) Advanced ester and formulated advanced ester.

(b) Super-refined naphthenic mineral oil and super-refined naphthenic mineral oil + 5 wt.% heavy resin.

Figure 2. - Viscosity as function of pressure for several lubricants using Roelands correlation (ref. 20).

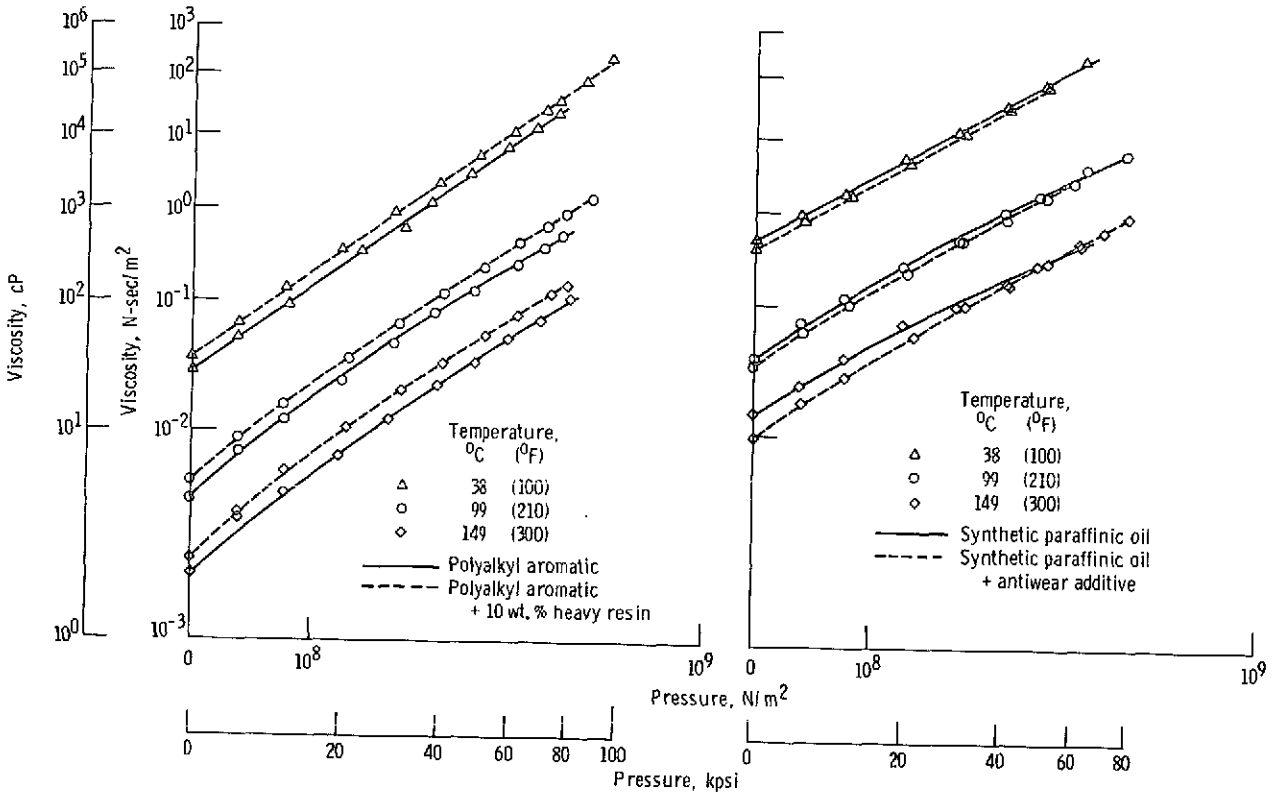

(c) Polyalkyl aromatic and polyalkyl aromatic + 10 wt. % heavy resin.

(d) Synthetic paraffinic oil (lot 3) and synthetic paraffinic oil (lot 2) + antiwear additive.

Figure 2. - Continued.

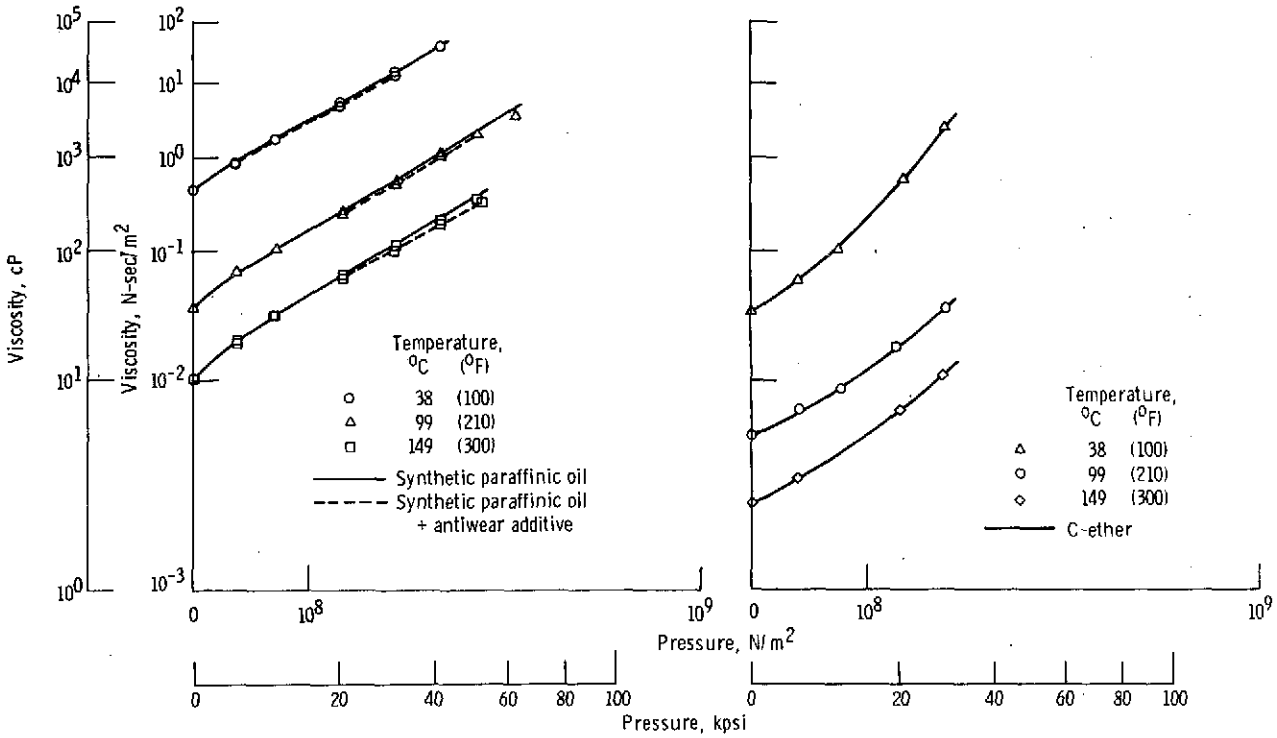

(e) Synthetic paraffinic oil (lot 4) and synthetic paraffinic oil (lot 4) + antiwear additive.

(f) C-ether.

Figure 2. - Continued.

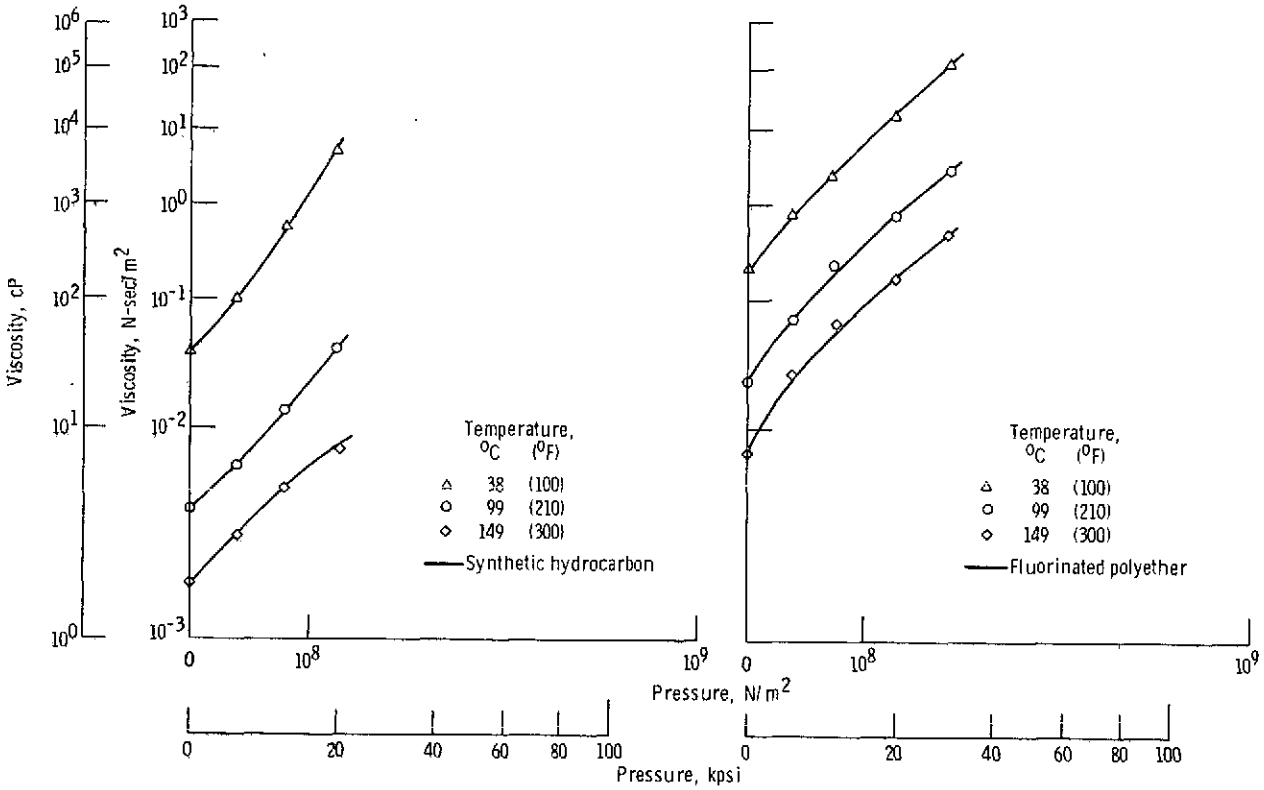

(g) Synthetic hydrocarbon (traction fluid).

(h) Fluorinated polyether.

Figure 2. - Concluded.

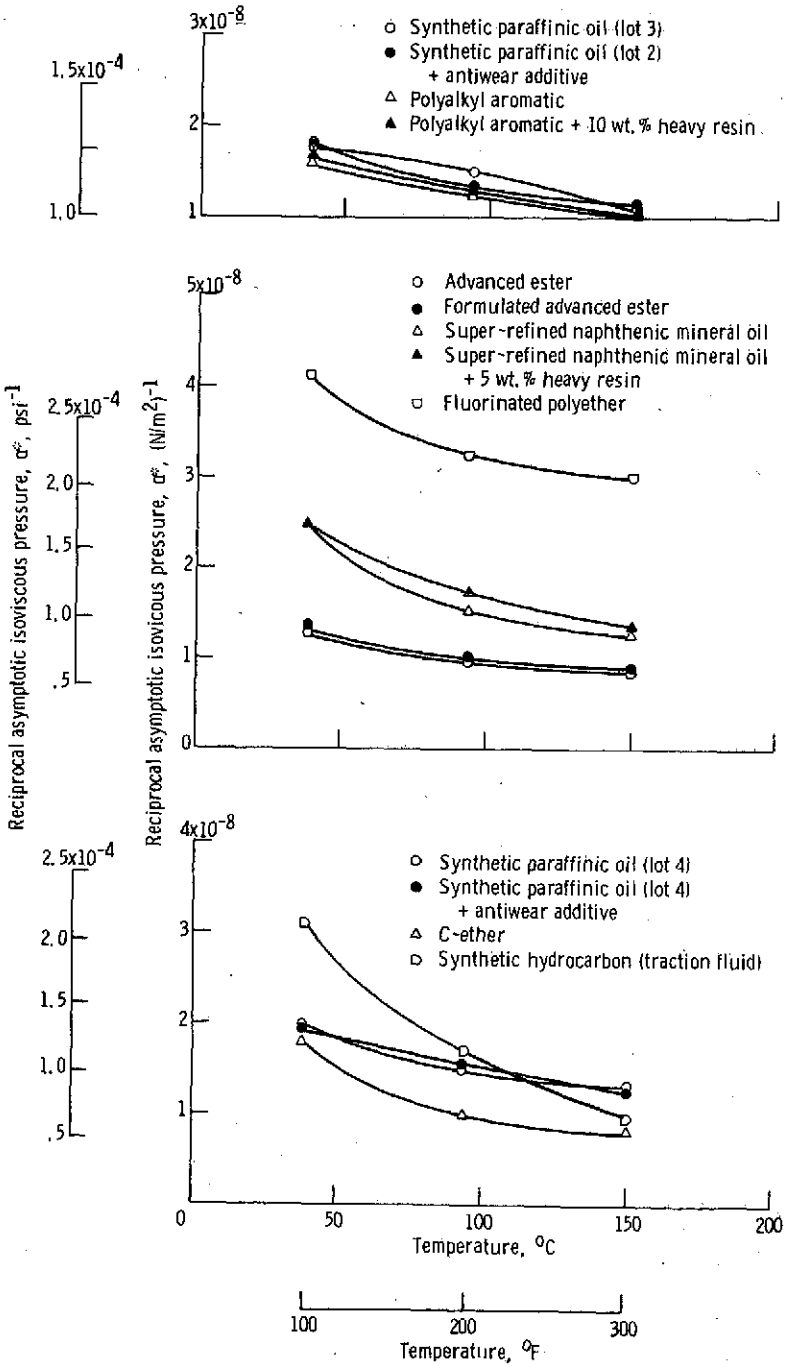

Figure 3. - Reciprocal asymptotic isoviscous pressure as function of temperature for several lubricants.

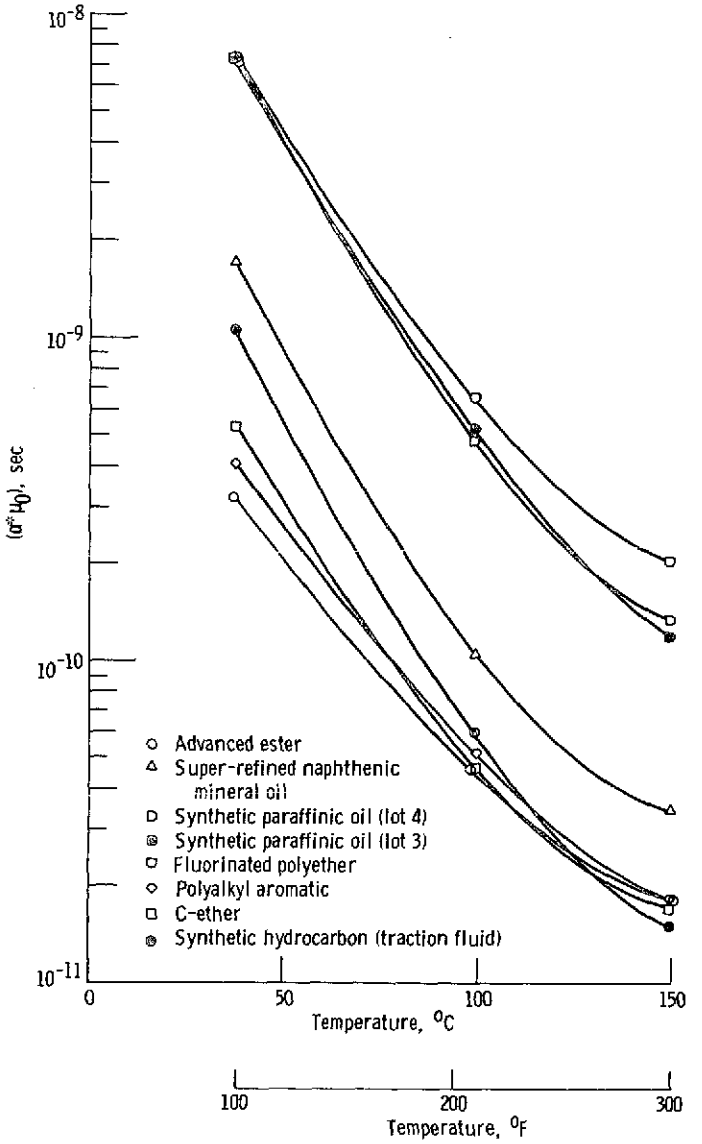

Figure 4. - EHD film forming capability as function of temperature for unformulated fluids.

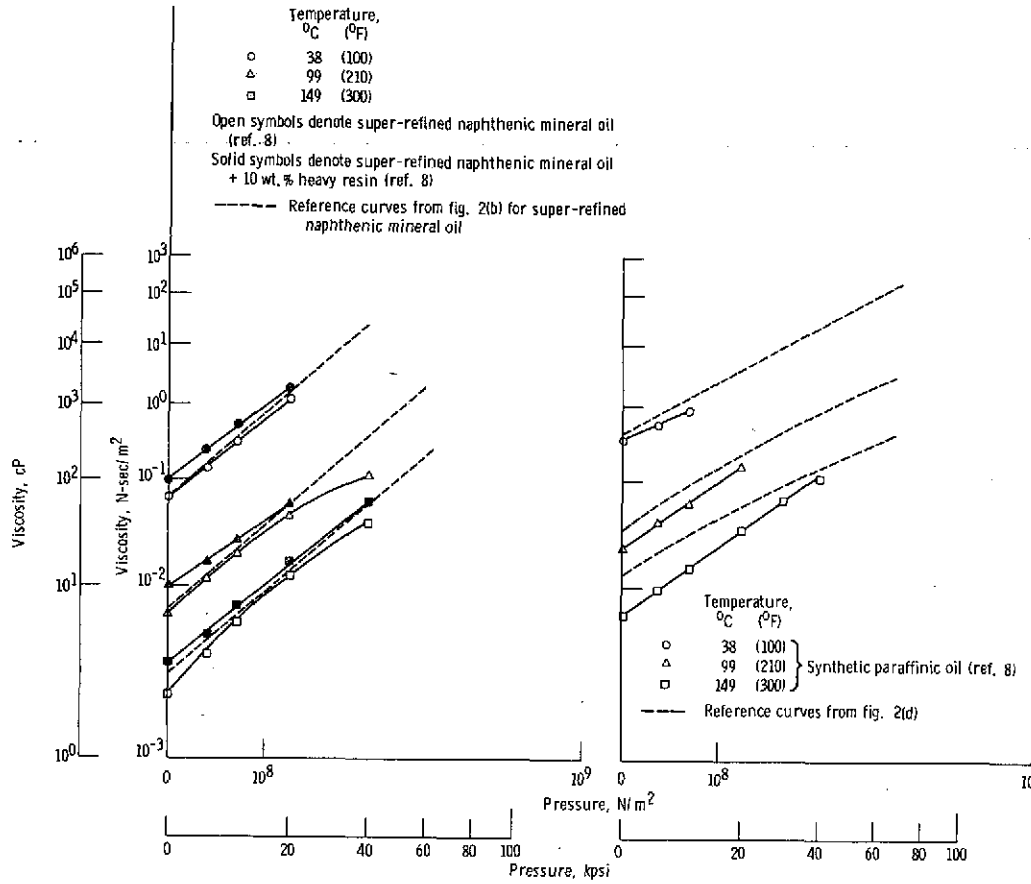

(a) Super-refined naphthenic mineral oil with and without heavy resin additive.

(b) Synthetic paraffinic oil (lot 3).

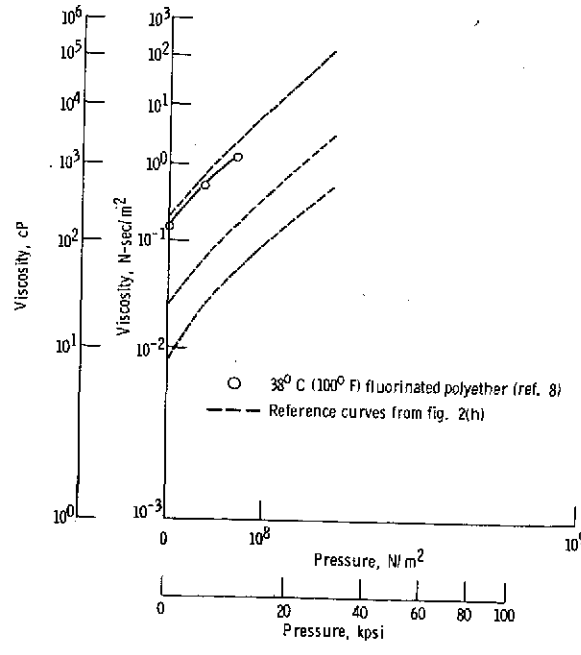

(c) Fluorinated polyether.

Figure 5. - Comparison of oscillating crystal (ref. 8) and capillary pressure viscosity data for four fluids.

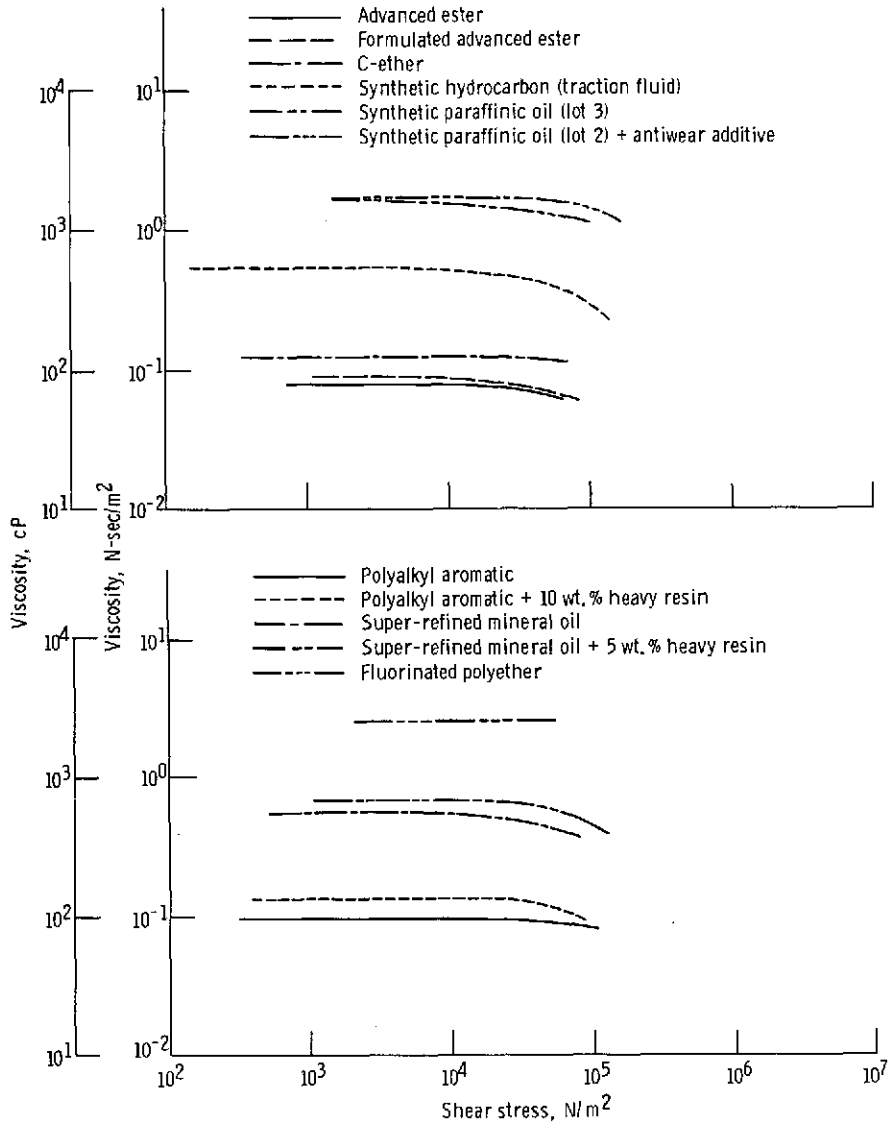

Figure 6. - Viscosity as function of shear stress for several lubricants. Temperature, 38° C (100° F); gage pressure, ~8.3x10^7 N/m^2 (12 000 psi).

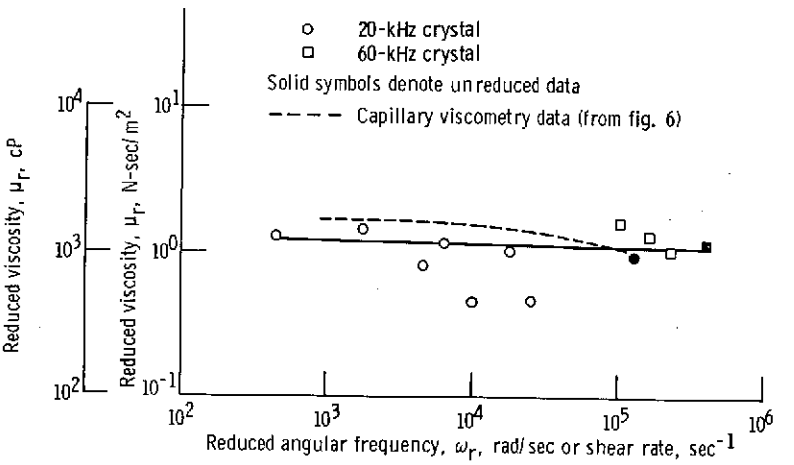

Figure 7. - Reduced viscosity as function of reduced angular frequency for synthetic paraffinic oil (lot 3). Reference temperature for reduced variable technique, 38^0 C (100^0 F); reference pressure for reduced variable technique, 6.9x10^7 N/m^2 (10^4 psi).

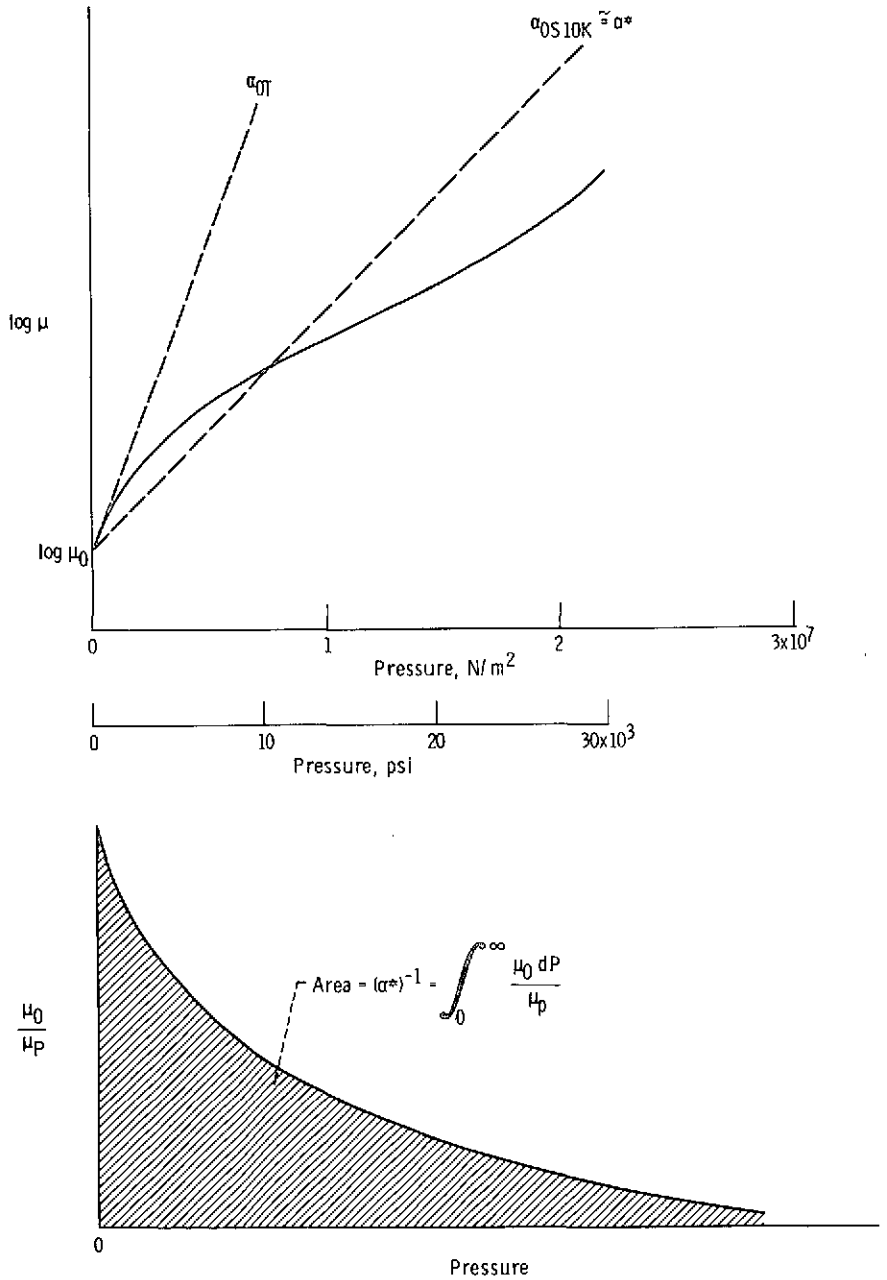

Figure 8. - Typical viscosity-pressure isotherm.

NASA-Langley, 1974 E-7952